Automation of the Spraying Process for Complex-shaped GFRC Panel Manufacturing

Hiroki Awaji[1], Akari Shimono[2], Kosuke Akita[3], Yasushi Ikeda[4]
[1,3]Asahi Building-Wall co. ltd [2,4]The University of Tokyo
[1,3]{hiroki-awaji|kosuke-akita}@agb.co.jp [2]simono-akari399@g.ecc.u-tokyo.ac.jp
[4]yasushi@arch1.t.u-tokyo.ac.jp

In recent years, the widespread use of parametric modeling software among designers has led to an increasing demand for complex-shaped elements. The glass fiber reinforced concrete (GFRC) spraying method has been used to create numerous complex-shaped panels. However, the growing complexity of shapes has increased the workload in manufacturing plants, while the number of skilled workers capable of executing the spraying process has been steadily declining. This study aims to automate the design of spray trajectory to establish a sustainable production system for complex-shaped GFRC panels. While previous research includes studies on spraying for double-curved formworks, plaster spraying, and shotcrete applications, few studies have focused on replicating the spraying processes of skilled workers using computer-aided design and simulation. First, to achieve this objective, the positions and angles of the spray gun over time were measured during the spraying process. Based on measurement data, the relationship between panel shape information and spraying conditions was inferred. Based on the spraying parameters estimated through measurement, a program was developed to automatically design spraying trajectories from the input of formwork geometry. Next, a simulation model was developed to calculate the thickness distribution of GFRC based on the spraying parameters. To identify the constants of this function, a spraying experiment was conducted, clarifying the relationship between the spraying parameters and the simulation constants. Furthermore, a program was developed to optimize the parameters of the trajectory design program by evaluating the error and uniformity of the thickness distribution generated by the simulation in comparison to the target shape. Through this process, an automatic design system of the spraying trajectory can be achieved, paving the way for the development of practical automated spraying machines and their implementation in architectural production.

Keywords: *automation, augmented reality, digital fabrication, GFRC manufacturing, robotic fabrication, shotcrete*

INTRODUCTION

Recent advancements in 3D CAD and visual programming tools have facilitated the design of complex architectural facades, including double-curved and multifaceted geometries. As a result, the demand for non-standard, uniquely shaped façade components has been increasing.

To realize such freeform facades, it is necessary to fabricate exterior panels with individually customized geometries. This represents a departure from conventional mass-

production models utilizing standardized molds and instead necessitates a production framework capable of high-mix, low-volume manufacturing.

Glass Fiber Reinforced Concrete (GFRC) has become a promising material for these applications. The Direct Spray Method, where glass fibers and mortar are sprayed onto custom molds, is commonly used to produce high-strength GFRC panels. Unlike traditional precast concrete, GFRC does not require steel reinforcement, allowing for thinner, lighter, and more intricate shapes. Projects like the Aomori Prefectural Sports Park Stadium (2018) and Azabudai Hills (2023) demonstrate the effectiveness of GFRC in complex façade designs (Figure 1) .

Figure 1
(a) Aomori Prefectural Sports Park Stadium (Kindaikenchiku-sha co., Ltd., 2018); (b) Azabudai Hills (Asahi Building-wall co., Ltd., 2023)

However, while digital tools have streamlined the design process, the increased complexity of geometries has significantly intensified the workload in production facilities. This has led to a growing shortage of skilled craftsmen capable of managing small-batch, high-variety production processes. As a result, the production capacity of GFRC panels is constrained, rendering it difficult to achieve productivity levels comparable to those of standardized mass production.

To address this issue, automation of the GFRC panel production process is necessary. For automation, the following two systems are essential; a formwork system that is repeatedly transformable into arbitrary curved surfaces by numerical input, and a spraying system that calculates appropriate spray paths based on the input formwork model and automatically executes spraying. This adaptive production system will enhance the production capacity of GFRC panels, which feature diverse curvatures. While examples of adaptive formwork systems have been demonstrated in fields outside GFRC, the development of automated spraying systems specifically tailored for GFRC has not progressed significantly. Such systems must consider the material properties of GFRC and incorporate the tacit knowledge of skilled spray technicians.

This paper focuses on the development of an automated spraying system, with the aim of establishing a production framework suitable for complex architectural facades under conditions of limited skilled labor.

Research purpose

This study aims to establish a sustainable production system for complex-shaped GFRC panels that does not rely on skilled labor, by automating the spraying process of the GFRC application method. Even for panels with highly complex geometries, the proposed system enables automatic calculation of the spraying path based on the design data, and execution of the spraying process using a robotic spraying system. This approach is expected to reduce the workload at the manufacturing site and mitigate dependency on experienced workers, thereby realizing a more efficient and flexible production process.

To achieve this, a design support program is developed to automatically generate optimal spraying paths for arbitrary panel geometries in accordance with the GFRC spraying method. The validity and practicality of the generated paths are then evaluated and verified.

Research method

In this study, we first conducted interviews with skilled craftsmen engaged in the Direct Spray Method to analyze their spraying processes and extract empirical rules underlying their operations. In parallel, we recorded the spraying trajectories using two different measurement techniques: AR

markers and motion sensors. By comparing the interview results with the measured trajectory data, we estimated the underlying rules of the spraying process.

Based on both the collected trajectory data and the inferred spraying rules from the interviews, we developed a computational program to generate spraying paths from the target surface geometry. Subsequently, we created a simulation program that takes the spraying path as input and outputs the resulting GFRC thickness distribution. The parameters of the simulator were identified by comparing simulated results with the actual thicknesses obtained from physical spraying tests. Finally, the spraying paths generated by the trajectory computation program were input into the simulator, and the simulated thickness distribution was compared with the target thickness of the actual product. Based on the discrepancies between the simulated and target thicknesses, we implemented a self-feedback mechanism that adjusts the parameters of the trajectory generation program.

Through this iterative process, comprising path computation, thickness simulation, and parameter adjustment—we aim to construct an automatic spraying path generation system that incorporates both the empirical knowledge of skilled craftsmen and the physical characteristics of the GFRC spraying process.

RELATED WORKS

Several previous studies have investigated the automation of spraying processes. P. Rennen et al. (2023) proposed an automated process for spraying and surface finishing on doubly curved formworks constructed using a cable-net formwork method. D. Mitterberger et al. (2022) developed a system in which an industrial robot performs plaster spraying along designer-defined paths, enabling a form of improvisational spraying. Y. Wang et al. (2024) developed a robot that automatically performs spraying and plastering, and proposed a method for quality inspection using LiDAR. N. Hack et al. (2020) introduced a construction method in which mortar is automatically sprayed onto rebar frameworks to create curved wall structures. J. McAlorum et al. (2021) introduced an automatic geopolymer spraying robot as a support system for concrete repair, where both skill and productivity are required. These studies demonstrate that substantial research has been conducted on implementing hardware systems for executing spraying tasks.

In contrast, studies aiming to replicate the spraying process of skilled craftsmen by measuring and analyzing their work and subsequently reproducing it through automated design and robotic control, remain scarce. Moreover, there are very few examples of design systems that incorporate a self-feedback mechanism—one that evaluates simulation results based on computed spraying paths and iteratively adjusts parameters to improve accuracy, as proposed in this study.

ANALYSIS OF SPRAY METHOD

In this study, a work analysis of skilled spraying workers was conducted to estimate various spraying parameters necessary for constructing a spraying simulator. The analysis involved two main methods: interviews with experienced workers and the measurement of spray gun trajectory data during actual spraying operations. The interviews provided an outline of the relationships among key parameters based on the craftsmen's experiential knowledge, while the trajectory measurements enabled the acquisition of detailed numerical data for further analysis.

Interview to the skilled craftsman

To understand how spraying parameters—such as spray velocity, distance, and angle—are determined, interviews were conducted with experienced craftsmen. The results revealed that these parameters are adjusted according to the

panel size. As the panel size increases, the spray must reach farther from the spray gun, resulting in a greater spray distance d. To maintain a relatively constant layer thickness per unit time, the spray velocity is reduced as the spray distance increases.

Regarding spray angles, it is generally desirable to spray perpendicularly to the surface of the formwork. However, in rising sections of the side formwork, maintaining a perpendicular angle is difficult; thus, craftsmen aim to spray at an angle as close to perpendicular as practicable.

Environmental factors such as temperature and humidity were also found to affect the spraying process. Higher temperature and humidity accelerate mortar hardening, requiring an increase in spray speed. In contrast, the hardness of the mortar was found to have little effect on the spraying parameters.

Measurement implementation

In this study, the spraying process performed by craftsmen was measured by OptiTrack. This tool is based on motion capture technology, which records the position and orientation by tracking reflection markers through multiple cameras. As shown in figure 2, reflection markers were attached to the spray gun. Additionally, markers were placed to record the position of the mold.

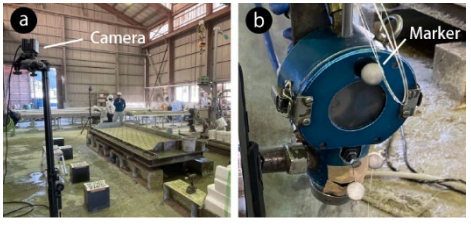

Figure 2
(a) Install tracking cameras around formwork; (b) Attach reflective markers to a spray gun

Spraying rules estimated from measurement

The average distance and from the formwork and average velocity were calculated from the position coordinates of the spray nozzle, recorded every 0.1 seconds by OptiTrack. The average distance was 416.05 mm, and the average velocity was 169.93 mm/s.

DEVELOPMENT OF SPRAY TRAJECTORY DESIGN PROGRAM

Based on the rules of spraying inferred from interviews with craftsmen and measurements of spray gun trajectories, a program was developed to calculate the spraying path for a desired panel surface geometry.

Overview of the program

The input to this program includes the product surface shape and the height of the edge rise. The spray parameters consist of the distance from the spray gun to the formwork surface (d [mm]), spray velocity (q [m/s]), spray angle (α [°]), spray range angle (β [°]), the offset distance (o [mm]) from the edge of the spray path, the spacing (p [mm]) between spray paths, and the radius of curvature (ρ [mm]) of the turnback points.

Estimation of the spraying parameters

The spraying parameters (d, q, α, β, o, p, ρ) were estimated through the following steps. First, the parameters α and β were assumed as follows. α is generally set to 90°, except for areas such as the side formwork where vertical spraying is not possible, where it is set to 45°. Additionally, β is assumed to be 25°, based on the results of the spraying experiment described later.

$$\alpha = \begin{cases} 90 & (formwork\ srf) \\ 45 & (side\ formwork\ srf) \end{cases} \qquad (1)$$
$$\beta = 25$$

Considering the mortar curing time, it is necessary to keep the total spraying time constant. Assuming the length of the trajectory is denoted as L [mm], the following equation is assumed:

$$\frac{L}{q} = const. \qquad (2)$$

From this, assuming the spraying speed and spraying trajectory length during measurement

are denoted as q_0 and L_0, the following equation is obtained:

$$q = \frac{L}{L_0} q_0 \quad (3)$$

The spraying pitch p is determined by the spraying range at a given distance d, so p is a function of d. Additionally, assuming $o = \rho = p/2$, L becomes a function of the side length w in the spraying direction and the spraying pitch p. Therefore, the following relation holds:

$$\begin{aligned} p &= f(d) \\ L &= g(w,p) = g'(w,d) \\ q &= h(d) \end{aligned} \quad (4)$$

From Equations (3) and (4), Equation (5) holds, which uniquely determines the spraying distance d. Furthermore, using this d, the other parameters (q, p, o, ρ) can also be determined. By executing this series of calculations using Rhino and Grasshopper, the spraying parameters can be determined automatically from the formwork geometry.

$$h(d) = \frac{g'(w,d)}{L_0} q_0 \quad (5)$$

Case study

Using the program developed in the previous section, a spray path was designed as a case study based on the assumed geometry of an actual panel that had been manufactured in the past. A semi-circular cross-sectional formwork was input as the formwork geometry. By using this spray design program, the position and angle vector of the spray gun at time t were automatically generated, as shown in figure 3.

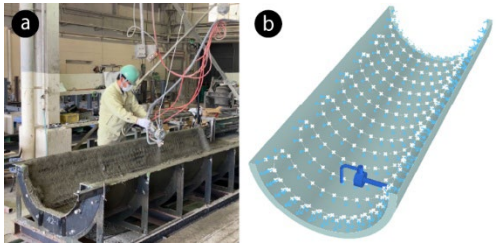

Figure 3
(a) Spraying on a semi-circular cross-sectional formwork; (b) the designed trajectory

DEVELOPMENT AND VALIDATION OF SPRAY SIMULATOR

Although the spray path calculation program developed in the previous chapter is based on empirically estimated rules derived from the craftsmen's experience, it does not directly consider the physical phenomena involved in the spraying process. Therefore, it is necessary to model the physical phenomena occurring during the spraying of mortar and glass fibers, and to simulate the relationship between the spraying path (velocity, angle, distance from the formwork surface) and the resulting thickness distribution of the GFRC panels.

To address this, the present study developed a simulator that takes as input the formwork surface, division numbers (u, v), the position of the nozzle (n_x, n_y, n_z), and the spray direction vector (v_x, v_y, v_z). The output of the simulator is the post-spray mortar layering model. Rhinoceros and Grasshopper were used to implement the simulator.

Calculation algorithm of spraying simulator

In this study, to represent the spray model in a 3DCG environment while preserving key spray characteristics, we develop a simulator based on two assumptions.

First, mortar is discharged radially from the nozzle and accumulates on the formwork surface as the nozzle moves. The trajectory of the discharged mortar can be approximated by a triangular pyramidal shape sharing a vertex. As illustrated in figure 4a, this spray volume is defined by the nozzle position and spray direction vector, with the spraying area determined by its intersection with the formwork.

Second, the spray model is assumed to consist of a finite number of box-shaped elements with uniform base area. Previous studies have reported that thickness distributions in spray-based applications can be approximated using a Gaussian function (Hongjian, 2020).

In this simulator, the thickness distribution is assumed to follow a Gaussian distribution, and the height of each box is calculated using equation (1).

$$f(x,y) = Ae^{-\left(\frac{(x-\mu_x)^2}{2\sigma_x{}^2}+\frac{(y-\mu_y)^2}{2\sigma_y{}^2}\right)} \quad (1)$$

A is the amplitude factor, which is linked to the height of the spraying-profile. σ is the standard deviation of the spraying-profile, which is related to sharpness. The center coordinate of spraying-profile on the formwork is described as $(\mu_x,\ \mu_y)$.

As shown in figure 4b, the formwork surface is divided based on the input values (u, v), and the spray model is simulated by extruding the surface in the normal direction within the spray area.

Continuous random variables can generally be discretized according to a specific rule. In this study, to simulate the mortar layering caused by nozzle movement, continuous spraying is represented by a series of spray models at arbitrary time t. As shown in figure 5, the mortar layering process is simulated by incrementally adding extrusion height at each time step.

The accuracy of the simulator improves with finer discretization of the formwork surface, but this increases computation time. Given that GFRC factory panels typically cover areas of around 10 m^2, simulating large-scale spraying with high accuracy necessitates reducing computational load. To address this, a breadth-first search (BFS) algorithm is employed. BFS, a graph search algorithm, explores nodes in order of proximity from the starting point.

First, the surface intersecting the spray direction vector is identified as the spraying center. Since the spray gun moves continuously, the current center is assumed to be near the previous one. Then, surface indices within the spray area are computed by searching from the center outward. This localized search significantly improves efficiency. By implementing these steps with BFS, the computational complexity is reduced from O(N^2) in brute-force search to O(N+M), enabling near-linear-time simulation.

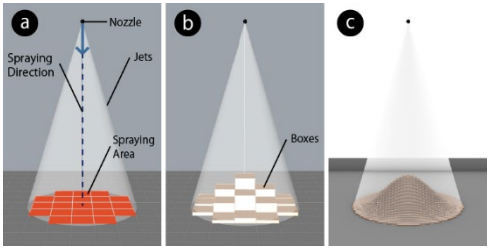

Figure 4
(a) Spraying model creation and surface extraction in spraying area; (b) Box creation; (c) High resolution spray model

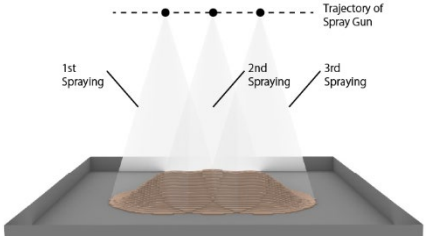

Figure 5
Continuous Spraying Model

Coefficients identification from experiment results

To determine the coefficients of equation (1), a skilled craftsman was asked to perform spraying operations as specified in table 1. After the spraying, the thickness distribution $d(u, v)$ was measured.

The operation parameters—spray time T [s], spray distance d [mm], and spray angle θ [deg]—were selected based on interviews with the craftsman, as these were considered influential to the resulting thickness. The tilt angle θ was defined as 90° when the spray direction vector was aligned with the surface normal vector.

The craftsman was instructed using a stopwatch for spray duration, a measuring tape for distance, and a protractor for angle adjustment. The size of each formwork used in the experiments was 900 x 900 mm.

In conditions A to C, the spraying gun was fixed at a designated position, and the craftsman

sprayed for a specified duration, repeated three times under each condition. Mortar thickness was measured after each spraying using a 3D scanner (Polycam Lidar Scanner) The pre-compaction thickness distribution $d\ (u\ , v\ )$ and the post-compaction thickness e measured separately (Figure 6).

Table 1
Operating parameters used for effect analysis

No.	T [s] × N [times]	d [mm]	θ [deq]
A-0	3.0 × 3	400	90
A-1	5.0 × 3	400	90
A-2	7.0 × 3	400	90
A-3	9.0 × 3	400	90
B-0	5.0 × 3	200	90
B-1	5.0 × 3	600	90
C-0	5.0 × 3	400	60
C-1	5.0 × 3	400	30

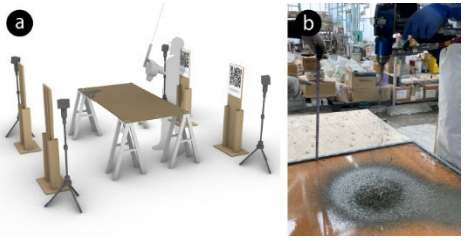

Figure 6
(a) Equipment for measurement; (b) spraying experiment

Gaussian fitting of spraying distribution

We determined the coefficients of equation (1) in the simulator from the measured data in the experiment. First, the gaussian fitting was performed on the thickness distribution from the 3D scan data of test specimens A-0 to A-3. The results of the Gaussian fitting for A-0 to A-3 are shown in figure 7a-b. A, σ_x, and σ_y increase in proportion to the spraying time, and the following approximate formulas are calculated respectively.

$$A_{d=400}(t) = 11.330t^{0.714} \quad (2)$$
$$\sigma_{x,d=400}(t) = 0.619t + 57.571 \quad (3)$$
$$\sigma_{y,d=400}(t) = 0.532t + 58.033 \quad (4)$$

The determination coefficient (R^2) for A is 0.948, suggesting that the prediction accuracy of the approximation formula is high. On the other hand, R^2 for σ_x and σ_y are low values, 0.271 and 0.274. These results are probably due to the movement of the spraying center caused by the craftsmen's manual spraying. Additional experiments, in which the spray gun is fixed using equipment, are being considered.

Gaussian fitting was also applied to the 3D scan data of B-0 and B-1 to calculate the rate of change relative to the reference distance $d = 400$ mm. The correlation of the spraying distance d and each coefficient is shown in figure 7c-d. R^2 for ξ_A, ξ_{σ_x} and ξ_{σ_y} are 0.911, 0.635, 0.910, indicating high prediction accuracy. The approximate formulas are the following:

$$\xi_A(d) = \frac{16.155}{0.049d} \quad (5)$$
$$\xi_{\sigma_x}(d) = 0.001d + 0.541 \quad (6)$$
$$\xi_{\sigma_y}(d) = 0.001d + 0.642 \quad (7)$$

Furthermore, we analyzed the 3D scan data of C-0 and C-1 to examine the correlation of the gaussian coefficients and a tilt of a spray gun. The result is shown in figure 7e-f. R^2 for ξ_A, ξ_{σ_x} and α_{σ_y} are 0.977, 0.382, 0.734. The prediction accuracy of ξ_A is considered high, but further experiments with larger number of samples for α_{σ_x} are necessary. The approximate formulas are the following:

$$\xi_A(\theta) = 0.011\theta + 0.030 \quad (8)$$
$$\xi_{\sigma_x}(\theta) = -0.007\theta + 1.701 \quad (9)$$
$$\xi_{\sigma_y}(\theta) = -0.018\theta + 2.574 \quad (10)$$

Based on the above analysis, the equation of spraying-thickness distribution can be expressed as below:

$$\varphi = B\int_0^T \left(\int A_{d=400}(t) e^{-\left(\frac{(x-\mu_x)^2}{2\sigma_x^2} + \frac{(y-\mu_y)^2}{2\sigma_y^2}\right)} dxdy \right) dt$$

Here, (11)

$$B = \xi_A(d)\xi_A(\theta)$$
$$\sigma_x = \xi_{\sigma_x}(d)\xi_{\sigma_x}(\theta)\sigma_{x,d=400}(t)$$
$$\sigma_y = \xi_{\sigma_y}(d)\xi_{\sigma_y}(\theta)\sigma_{y,d=400}(t)$$

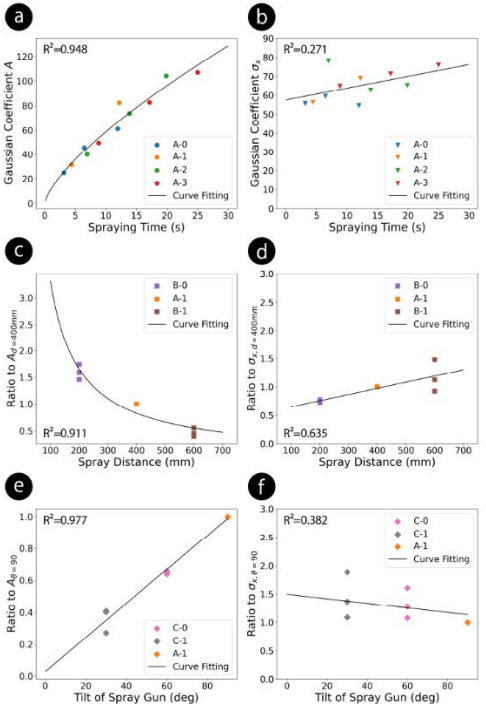

Figure 7
Results of the coefficient from gaussian fitting
(a) A; (b) σ_x;
(c) $\xi_A(d)$; (d) $\xi_{\sigma_x}(d)$;
(e) $\xi_A(\theta)$; (f) $\xi_{\sigma_x}(\theta)$

Finally, a comparison of the simulation and the experimental data was conducted. The simulation used the position and tilt data of the spray gun recorded during the experiment described above. As shown in figure 8, the experimental results closely match the simulation ones. The error analysis results are presented in Table 2. A total of 17 datasets, for which both the spray gun operation records and 3D scan data were successfully obtained (A-0: 3, A-1: 2, A-2: 3, A-3: 3, B-0: 3, B-1: 3), were analyzed. For each dataset, the resulting geometry was divided into three regions based on height: the lower 33% (foothill), the middle 33% (mid-slope), and the upper 33% (summit). The mean absolute error (MAE) between the 3D scan data and the simulation results was then calculated for each region. Furthermore, for each experimental condition group, the MAE values from individual trials were averaged to obtain a representative value for that group. Overall, the simulation results generally agreed with the measured data, demonstrating a certain degree of reproducibility. However, in some cases, discrepancies were observed that may be attributed to measurement errors in the spray gun operation records or outliers in the 3D scan data. To more rigorously quantify these sources of error, further accumulation of data and statistical analysis will be required in future studies.

No.	foothill	mid-slope	summit
A-0	2.255	3.442	8.536
A-1	1.677	5.803	11.399
A-2	4.475	9.058	20.583
A-3	3.526	6.190	16.881
B-0	5.508	8.110	3.938
B-1	2.243	4.898	3.007

Table 2:
MAE (mm) comparison with simulated results and experiment ones

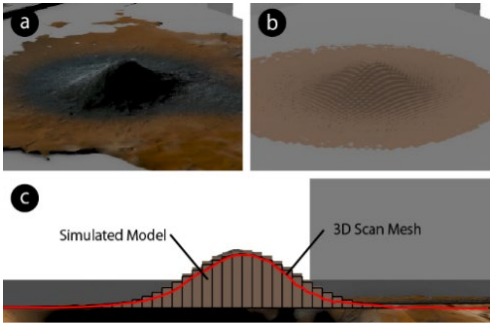

Figure 8:
(a) Experiment result (B-01); (b) Simulation output (B-01);
(c) Section Comparison (B-01)

OPTIMIZATION OF SPRAYING PARAMETERS

By using the spray path program and thickness distribution analysis program developed in this study, it is possible to estimate the thickness distribution resulting from spraying by inputting a target surface. The deviation from the target thickness and the uniformity of the thickness distribution are evaluated based on this estimated data. Then, by optimizing spraying parameters

such as spray distance and spray speed to minimize these two objective functions, the final spraying parameters are determined.

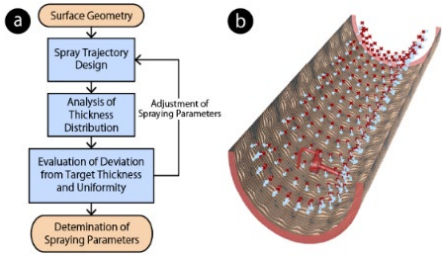

Figure 9
(a) Spraying trajectory design process; (b) case study with simulation and optimization

Evaluation of trajectory calculation through spray simulation

As a case study, the thickness distribution on a semi-circular cross-section formwork was calculated and evaluated to optimize the spray distance and spray speed (Figure 9). The initial parameters prior to optimization were obtained using the spray path design program. The objective function was defined as the product of the error E [mm] between the average compressed thickness and the target thickness, and the standard deviation σ of the thickness across the formwork. The objective function f is given as:

$$f = E \cdot \sigma \qquad (1)$$

An optimization program was implemented in Rhino + Grasshopper to minimize this objective function *f*. Through this process, the optimal spraying parameters that achieve a thickness distribution closest to the target and most uniform for the semi-circular cross-section formwork were successfully determined.

CONCLUSION

In this study, we first conducted interviews with skilled spray craftsmen and measured their spraying trajectory to roughly estimate key spraying parameters such as spray distance, speed, and angle. Based on these estimated parameters, we then developed a program that designs spraying trajectories from the input formwork surface geometry. Furthermore, we created a simulation model that calculates the GFRC panel thickness distribution resulting from a given spraying trajectory and identified detailed model parameters through experiments.

Finally, by inputting the trajectory data generated from the spraying trajectory design program into the simulation, we evaluated the error and uniformity of the resulting thickness distribution compared to the target thickness. Through optimization of the parameters in the spraying trajectory design program, we demonstrated that it is possible to determine spraying parameters that achieve the desired panel thickness.

At this stage, there are still many unknowns in determining the optimal toolpath. As a preparatory step toward analyzing what constitutes an optimal toolpath, this study developed a simulation method and verified its consistency with actual results. This alignment between simulation and physical outcomes can be considered one of the key achievements of the research.

FUTURE PROSPECT

As a future prospect, it is necessary to perform actual spraying based on parameters obtained through the design, simulation, and optimization process. The resulting thickness distribution should be measured and compared with both simulation results and those from manual spraying by skilled workers. This comparison will help refine trajectory parameters to better reflect physical behavior and improve accuracy. In this study, semi-cylindrical panels from an actual project were used; however, the effectiveness of the simulation is expected to improve further when applied to more complex geometries, such as doubly curved surfaces, in full-scale spraying tests.

In addition, due to variations in temperature and humidity, the flowability of mortar changes,

which in turn affects the spraying velocity and the distance from the formwork surface. Therefore, it is necessary to develop a program that incorporates such environmental conditions as simulation parameters. Regarding the thickness parameter, this study assumes a uniform thickness. However, in the future, it may be possible to optimize thickness based on stress distribution—for instance, increasing the thickness in central areas subject to higher wind pressure compared to the edges—to minimize cement usage.

This research ultimately aims to develop a system in which the formwork automatically adapts to the desired panel shape, the spraying gun trajectory is automatically calculated from the panel's geometry data, and the spraying process is executed by an automated spraying machine (Figure 10). Such a system would enable the systematic production of complex-shaped GFRC panels without relying on skilled labor, thereby paving the way for the development and implementation of automated spraying machines in actual architectural fabrication.

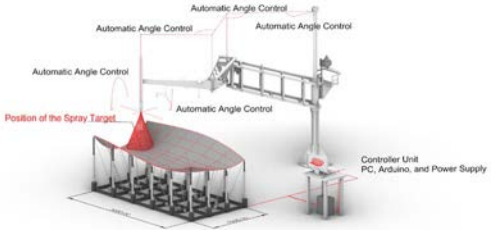

Figure 10 Conceptual Diagram of an Automated Spraying System for Complex-Shaped Panels

REFERENCES

Kindaikenchiku-sha co., Ltd. (2018) *Aomori Prefectural Sports Park Stadium* [online]. Available at: http://www.kindaikenchiku.co.jp/pr1_details/20201106173806_13.html (Accessed: 29 March 2025)

Asahi Building-wall co., Ltd. (2023) *Azabudai Hills* [online]. Available at: https://www.agb.co.jp/works/detail/?id=1400 (Accessed: 29 March 2025)

Philipp, R., et al. (2023) 'Robotic Knitcrete: Computational Design and Fabrication of a Pedestrian Bridge Using Robotic Shotcrete on a 3D-Knitted Formwork', *Frontiers in Built Environment,* 9, pp. 1-18. Available at: https://doi.org/10.3389/fbuil.2023.1269000 (Accessed: 29 March 2025)

Daniela, M., et al. (2022) 'Interactive Robotic Plastering: Augmented Interactive Design and Fabrication for On-site Robotic Plastering', *Proceedings of the 2022 CHI Conference on Human Factors in Computing Systems*, 174, pp.1-18. Available at: https://dl.acm.org/doi/10.1145/3491102.3501842 (Accessed: 29 March 2025)

Yue, W. et al. (2024) 'Mortar Spraying and Plastering Integrated Robot for Wall Construction', *Automation in Construction*, 165, pp. 1-14. Available at: https://doi.org/10.1016/j.autcon.2024.105533 (Accessed: 29 March 2025)

Hack, N. and Kloft, H. (2020) 'Shotcrete 3D Printing Technology for the Fabrication of Slender Fully Reinforced Freeform Concrete Elements with High Surface Quality: A Real-Scale Demonstrator', *Second RILEM International Conference on Concrete and Digital Fabrication, 28,* pp.1128-1137. Available at: https://doi.org/10.1007/978-3-030-49916-7_107 (Accessed: 29 March 2025)

Jack. M., et al. (2021) 'Robotic Spray Coating of Self-sensing Metakaolin Geopolymer for Concrete Monitoring', *Automation in Construction*, 121, pp.1-7. Available at: https://doi.org/10.1016/j.autcon.2020.103415 (Accessed: 29 March 2025)

Hongjian, W., et al. (2020) 'A New Approach to Simulate Coating Thickness in Cold Spray', *Surface and Coatings Technology,* 382 pp.1-14. Available at: https://doi.org/10.1016/j.surfcoat.2019.125151 (Accessed: 29 March 2025)